Available online at www.sciencedirect.com
SCIENCE DIRECT®
Inorganica Chimica Acta 357 (2004) 294–300
Inorganica Chimica Acta
www.elsevier.com/locate/ica

New dinuclear Co(II) and Mn(II) complexes of the phenol-based compartmental ligand containing formyl and amine functions: structural, spectroscopic and magnetic properties

Iryna A. Koval [a], Mieke Huisman [a], Arno F. Stassen [a], Patrick Gamez [a], Martin Lutz [b], Anthony L. Spek [b], Daniel Pursche [c], Bernt Krebs [c], Jan Reedijk [a,*]

[a] *Leiden University, Leiden Institute of Chemistry, P.O. Box 9502, 2300 RA Leiden, The Netherlands*
[b] *Bijvoet Centre for Biomolecular Research, Crystal and Structural Chemistry, Utrecht University, Padualaan 8, 3584 CH Utrecht, The Netherlands*
[c] *Institut für Anorganische und Analytische Chemie der Westfälischen Wilhelms-Universität Münster, Wilhelm-Klemm-Straße 8, D-48149 Münster, Germany*

Received 18 June 2003; accepted 20 June 2003

Abstract

The phenol-based compartmental ligand Hpy2ald contains a tridentate amino arm and a weak donor aldehyde group at the 2′ and at the 6′ positions of the phenol ring, respectively. This ligand reacts with cobalt(II) perchlorate, cobalt(II) tetrafluoroborate and manganese(II) perchlorate, yielding dinuclear complexes, where two metal ions are doubly bridged by two deprotonated cresolate moieties. The coordination environment around the metal ions is then completed to a very distorted octahedron by three nitrogen donor atoms from the pendant amino arm and the oxygen atom of the aldehyde group. The crystal structures of the complexes, their spectroscopic and magnetic properties are reported.

Keywords: Cobalt; Manganese; Dinuclear; Magnetism

1. Introduction

The term ''dinucleating ligands'' was first introduced in 1970 by Robson [1] to describe the class of polydentate chelating ligands, able to bind simultaneously two metal ions. Since then, a very large number of such ligands were designed, and their coordination compounds were thoroughly investigated. The possible applications of the complexes with this type of ligands vary from modeling the active sites of many metalloenzymes [2–4], to hosting and carrying small molecules [5–7] or catalysis [8,9].

Among many different types of dinucleating ligands, the phenol-based compartmental ligands attracted particularly wide attention of scientists. The term ''compartmental'' was introduced to indicate a ligand containing two adjacent, but dissimilar coordination sites [2]. Particular interest in this type of ligands resulted from the recent recognition of the asymmetric nature of a number of dimetallic biosites [10,11]. Understanding of the ability of individual metal ions to play possibly different functions in dinuclear sites in metalloenzymes led to the design of a great number of asymmetric ligands where two compartments would provide a different coordination surrounding for the two metal ions.

In the present study, three novel complexes obtained from cobalt(II) and manganese(II) and the phenol-based ligand Hpy2ald are described. All complexes contain a dinuclear metal core, where two metal ions are doubly bridged by two oxygen atoms from two deprotonated cresolate moieties. Crystal structures, spectroscopic and magnetic properties of these complexes are reported.

* Corresponding author. Tel.: +715274450; fax: +715274671.
E-mail address: reedijk@chem.leidenuniv.nl (J. Reedijk).

0020-1693/$ - see front matter © 2003 Elsevier B.V. All rights reserved.
doi:10.1016/S0020-1693(03)00422-5

2. Experimental

2.1. Materials and methods

All starting materials were commercially available and used as purchased. The proligand Hpy2ald was synthesized as previously described [12]. The infrared spectra of the complexes in the 4000–300 cm^{-1} range were recorded on a Bruker 330V IR spectrophotometer equipped with a Golden Gate Diamond. The ligand field spectra of the solids (300–2000 cm^{-1}, diffuse reflectance) and in solution were taken on a Perkin–Elmer 330 spectrophotometer equipped with a data station. Bulk magnetizations of polycrystalline samples were measured in the range 5–300 K with a Quantum Design MPMS-5S SQUID magnetometer, in a 1 kG applied field. The data were corrected for the experimentally determined contribution of the sample holder. Corrections for the diamagnetic responses of the complexes, as estimated from Pascal's constants, were applied [13].

Caution: although no difficulties was encountered while working with perchlorate complexes, they are potentially explosive and should be handled with care.

2.2. Preparation of the complexes

2.2.1. $[Co_2(py2ald)_2](ClO_4)_2 \cdot 0.7CH_3OH$ (1)

Twenty milliliters of a methanol solution of cobalt(II) perchlorate (146 mg, 0.4 mmol) were added to 20 ml of a methanol solution of the ligand (69 mg, 0.2 mmol). Slow evaporation of the solvent yielded pink rectangular crystals suitable for X-ray crystal structure determination. Elemental analysis for $C_{42.7}H_{42.8}Cl_2Co_2N_6O_{12.7}$, found (calc.): C, 49.3 (49.7); H, 4.0 (4.2); N, 8.1% (8.0). IR, cm^{-1}: 3567 (O–H stretching); 2898 (C–H stretching); 1635 (C=O stretching); 1606, 1557 (C=N arom., C=C arom.), 1080 (ClO_4^-).

2.2.2. $[Co_2(py2ald)_2](BF_4)_2 \cdot CH_3OH$ (2)

Twenty milliliters of a methanol solution of cobalt(II) tetrafluoroborate (136 mg, 0.4 mmol) were added to 20 ml of a methanol solution of the ligand (69 mg, 0.2 mmol). Slow ether diffusion into the resulting pink solution yielded small pink hexagonal crystals of the complex which were found to be suitable for X-ray crystal structure determination. Elemental analysis for $C_{43}H_{43}B_2Co_2F_8N_6O_3$, found (calc.): C, 50.6 (50.8); H, 4.4 (4.4); N, 8.5% (8.3). IR, cm^{-1}: 2916 (C–H stretching); 1635 (C=O stretching); 1607, 1558 (C=N arom., C=C arom.); 1032 (BF_4^-).

2.2.3. $[Mn_2(py2ald)_2](ClO_4)_2 \cdot C_4H_{10}O$ (3)

A solution of manganese(II) perchlorate (245 mg, 0.4 mmol) in 20 ml of methanol was added to a solution of the ligand (69 mg, 0.2 mmol) in 20 ml of methanol. Ether diffusion into the resulting bright-yellow solution led to the appearance of yellow rod-shaped crystals which were found suitable for X-ray crystal structure determination. Crystals were found to deteriorate rapidly while taken out of the mother solution, due to the loss of ether molecules from the crystal lattice. Elemental analysis for $C_{42}H_{40}Cl_2Mn_2N_6O_{12}$, found (calc.): C, 50.1 (50.4); H, 4.0 (4.0), N, 8.4% (8.4). IR, cm^{-1}: 2924 (C–H stretching); 1643 (C=O stretching); 1602, 1554 (C=N arom., C=H arom.), 1079 (ClO_4^-).

2.3. Crystal structure determinations

Crystal data for compound **1**: $(C_{42}H_{40}Co_2N_6O_4)(ClO_4)_2 \cdot 0.7(CH_4O)$, Fw = 1031.99, red–brown block, $0.30 \times 0.25 \times 0.18$ mm^3, orthorhombic, *Fdd*2 (no. 43), $a = 27.0312(2)$ Å, $b = 34.1008(2)$ Å, $c = 18.9101(1)$ Å, $V = 17431.05(19)$ $Å^3$, $Z = 16$, $D_x = 1.573$ g/cm^3. 66 127 reflections were measured on a Nonius KappaCCD diffractometer with rotating anode ($\lambda = 0.71073$ Å) at a temperature of 150(2) K up to a resolution of $(\sin\theta/\lambda)_{max} = 0.61$ $Å^{-1}$; 8090 reflections were unique ($R_{int} = 0.040$). An absorption correction based on multiple measured reflections was applied ($\mu = 0.957$ mm^{-1}, 0.73–0.78 transmission). The structure was solved with Patterson methods (DIRDIF-97 [14]) and refined with SHELXS 97 [15] against F^2 of all reflections. Non-hydrogen atoms were refined freely with anisotropic displacement parameters. One perchlorate anion was refined with a disorder model. H atoms were refined as rigid groups; methanol H atoms were kept fixed. 634 refined parameters, 52 restraints. Flack x-parameter [16]: 0.005(9). R values [$I > 2\sigma(I)$]: $R1 = 0.0285$, $wR2 = 0.0784$. R values [all refl.]: $R1 = 0.0318$, $wR2 = 0.0806$. GoF = 1.040. Residual electron density between −0.36 and 0.46 e/$Å^3$. Molecular illustration, structure checking and calculations were performed with the PLATON package [17].

Crystal data for compound **2**: $(C_{42}H_{40}Co_2N_6O_4)(BF_4)_2(CH_4O)$, Fw = 1016.32, brown block, $0.21 \times 0.15 \times 0.09$ mm^3, orthorhombic, *Fdd*2 (no. 43), $a = 26.8533(2)$ Å, $b = 33.8399(3)$ Å, $c = 18.8585(1)$ Å, $V = 17137.0(2)$ $Å^3$, $Z = 16$, $D_x = 1.576$ g/cm^3. 55 275 reflections were measured on a Nonius KappaCCD diffractometer with rotating anode ($\lambda = 0.71073$ Å) at a temperature of 150(2) K up to a resolution of $(\sin\theta/\lambda)_{max} = 0.59$ $Å^{-1}$; 7384 reflections were unique ($R_{int} = 0.053$). An absorption correction based on multiple measured reflections was applied ($\mu = 0.863$ mm^{-1}, 0.85–0.92 transmission). Coordinates of compound **1** were taken as starting model and refined with SHELXS 97 [15] against F^2 of all reflections. Non-hydrogen atoms were refined freely with anisotropic displacement parameters. One BF_4 anion was refined with a disorder model. H atoms were refined as rigid groups. 608 refined parameters, 40 restraints. Flack x-parameter [16]:

−0.026(11). R values [$I > 2\sigma(I)$]: $R1 = 0.0335$, $wR2 = 0.0790$. R values [all refl.]: $R1 = 0.0411$, $wR2 = 0.0828$. GoF = 1.017. Residual electron density between −0.44 and 0.71 e/Å^3. Molecular illustration, structure checking and calculations were performed with the PLATON package [17].

Crystal data for compound **3**: $(C_{42}H_{40}Mn_2N_6O_4)(ClO_4)_2(C_4H_{10}O)$, Fw = 1075.20, yellow block, 0.1 × 0.1 × 0.04 mm^3, triclinic, $P\bar{1}$ (no. 2), $a = 12.6517(3)$ Å, $b = 12.7867(3)$ Å, $c = 16.7288(4)$ Å, $\alpha = 85.068(2)°$, $\beta = 75.6270(10)°$, $\gamma = 65.4720(10)°$, $V = 2384.55(10)$ Å^3, $Z = 2$, $D_x = 1.497$ g/cm^3. 14 022 reflections were collected on a Bruker AXS Smart 6000 CCD diffraction system using Cu radiation ($\lambda = 1.54178$ Å) at a temperature of 153 K; 8009 reflections were unique ($R_{int} = 0.0390$). The structure was solved by direct methods using the program SHELXS 97 [15]. The final positions of all non-hydrogen atoms were taken from a series of full-matrix least-squares refinement cycles based on F^2 with the SHELXS 97 program followed by difference Fourier synthesis [15]. All non-hydrogen atoms, the counter ions and the ether solvent molecule were refined anisotropically. All hydrogen atoms were placed on calculated positions and allowed to ride on their corresponding atoms. The isotropical thermal parameters for the methyl protons were refined with 1.5 times and for all other hydrogen atoms with 1.2 times of the U_{eq} value of the bonding atom. 624 refined parameters, 0 restraints. R values [$I > 2\sigma(I)$]: $R1 = 0.0516$, $wR2 = 0.1307$. R values [all refl.]: $R1 = 0.0706$, $wR2 = 0.1379$. GoF = 0.959. Residual electron density between −0.67 and 0.91 e/Å^3.

CCDC 212530 (compound **1**), 212531 (**2**) and 212532 (**3**) contain the supplementary crystallographic data for this paper. These data can be obtained free of charge via www.ccdc.cam.ac.uk/conts/retrieving.html (or from the CCDC, 12 Union Road, Cambridge CB2 1EZ, UK; fax: +44 1223 336033; e-mail: deposit@ccdc.cam.ac.uk).

3. Results and discussion

3.1. General

The ligand Hpy2ald was prepared as an intermediate in the synthesis of asymmetric dinucleating ligands [12]. It contains a tridentate pendant arm in the 2′ position of the phenol ring and an aldehyde group in the 6′ position of the phenol ring. The reactions of Hpy2ald with cobalt and manganese salts of weakly coordinating or non-coordinating anions, such as ClO_4^- or BF_4^-, yield dinuclear complexes with the metal to ligand ratio of 2:2. In all complexes, each metal ion is coordinated by three nitrogen donor atoms of a pendant arm, two oxygen atoms from deprotonated cresolate moieties and the oxygen atom of the formyl group. Ni(II) complexes with similar structures were previously described by Fenton and co-workers [18]. However, in those cases, the formyl-containing ligands were generated in situ due to the hydrolysis of one of the two pendant arms from the initial ligands.

3.2. Crystal structure descriptions

3.2.1. $[Co_2(py2ald)_2](ClO_4)_2 \cdot 0.7CH_3OH$ (1)

Pink rectangular blocks of the compound were obtained by diethyl ether diffusion into the methanol solution of the reactants. The Platon [17] projection of the complex cation $[Co_2(py2ald)_2]^{2+}$ is shown in Fig. 1. Selected bond lengths and angles are presented in Table 1. The compound crystallizes in the space group *Fdd2*, with 16 formula units present per unit cell. The complex cation is constituted by two deprotonated ligands and two Co(II) ions, resulting in a dimeric dinuclear structure with a Co···Co separation of 3.2031(6) Å. Two cobalt ions are bridged by two μ-phenoxy bridges from two deprotonated cresolates, resulting in an almost ideal parallelogram formed by two *trans*-located cobalt ions Co1 and Co2 and two *trans*-located oxygen atoms O31 and O71. The distances Co1–O71 and Co2–O31 are approximately equal (2.0323(19) and 2.0344(19) Å, respectively), as well as the distances Co1–O31 and Co2–O71 (2.100(2) and 2.101(2) Å, respectively). The

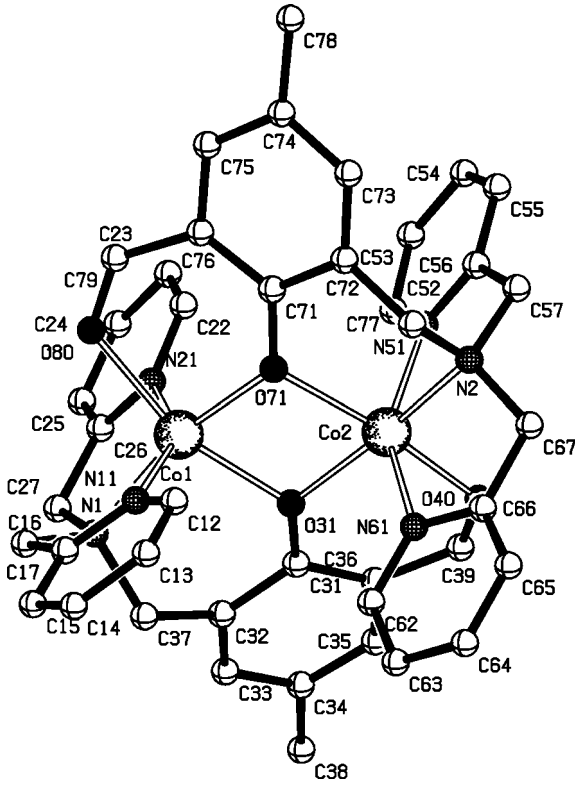

Fig. 1. Platon [17] projection of the complex cation $Co_2(py2ald)_2]^{2+}$. Hydrogen atoms are omitted for clarity.

Table 1
Selected bond lengths and bond angles for $[Co_2(py2ald)_2](ClO_4)_2 \cdot 0.7CH_3OH$

Bond lengths (Å)			
Co(1)–N(11)	2.118(2)	Co(2)–N(51)	2.111(2)
Co(1)–N(21)	2.121(2)	Co(2)–N(61)	2.111(2)
Co(1)–N(1)	2.171(2)	Co(2)–N(2)	2.168(2)
Co(1)–O(31)	2.100(2)	Co(2)–O(31)	2.0343(18)
Co(1)–O(71)	2.0325(18)	Co(2)–O(71)	2.101(2)
Co(1)–O(80)	2.157(2)	Co(2)–O(40)	2.141(2)
Bond angles			
O(31)–Co(1)–O(71)	78.32(7)	O(31)–Co(2)–O(40)	87.97(8)
O(31)–Co(1)–O(80)	162.24(7)	O(31)–Co(2)–O(71)	78.25(8)
O(31)–Co(1)–N(1)	91.61(9)	O(31)–Co(2)–N(2)	166.29(8)
O(31)–Co(1)–N(11)	103.97(8)	O(31)–Co(2)–N(51)	111.58(8)
O(31)–Co(1)–N(21)	95.94(9)	O(31)–Co(2)–N(61)	94.43(8)
O(71)–Co(1)–O(80)	87.41(8)	O(40)–Co(2)–O(71)	162.73(7)
O(71)–Co(1)–N(1)	165.10(8)	O(40)–Co(2)–N(2)	102.95(8)
O(71)–Co(1)–N(11)	93.04(8)	O(40)–Co(2)–N(51)	82.18(9)
O(71)–Co(1)–N(21)	113.45(8)	O(40)–Co(2)–N(61)	86.69(9)
O(80)–Co(1)–N(1)	104.30(9)	O(71)–Co(2)–N(2)	92.30(8)
O(80)–Co(1)–N(11)	87.14(9)	O(71)–Co(2)–N(51)	93.16(8)
O(80)–Co(1)–N(21)	79.97(10)	O(71)–Co(2)–N(61)	104.54(8)
N(1)–Co(1)–N(11)	78.62(9)	N(2)–Co(2)–N(51)	78.52(9)
N(1)–Co(1)–N(21)	78.20(8)	N(2)–Co(2)–N(61)	78.20(9)
N(11)–Co(1)–N(21)	149.70(9)	N(51)–Co(2)–N(61)	151.16(9)

interior angles of the parallelogram are 78.32(7)° and 78.25(8)° for O–Co–O and 101.57(8)° and 101.55(9)° for Co–O–Co, and their sum amounts to 359.7°, which is very close to the planar value of 360°.

Both cobalt ions have a significantly distorted octahedron surrounding, accomplished by a N_3O_3 donor set. The coordination sphere of each ion is completed by two nitrogen atoms from two pyridine rings, a nitrogen donor from a tertiary amine group and an oxygen from the carbonyl group. For both ions, the oxygen atom from the deprotonated cresolate and the nitrogen atom from the tertiary amine group are occupying the axial positions, whereas two pyridine rings lie in the equatorial plane on either side of the ligand plane and thus are *trans*-located to each other.

The doubly positive charge of the complex cation is compensated by perchlorate anions. One perchlorate is on a general position and two independent perchlorates

Table 2
Selected bond lengths and bond angles for $[Co_2(py2ald)_2](BF_4)_2 \cdot CH_3OH$

Bond lengths (Å)			
Co(1)–N(11)	2.112(3)	Co(2)–N(51)	2.099(3)
Co(1)–N(21)	2.124(3)	Co(2)–N(61)	2.105(3)
Co(1)–N(1)	2.174(3)	Co(2)–N(2)	2.168(3)
Co(1)–O(31)	2.100(3)	Co(2)–O(31)	2.033(2)
Co(1)–O(71)	2.033(2)	Co(2)–O(71)	2.094(2)
Co(1)–O(80)	2.161(3)	Co(2)–O(40)	2.146(2)
Bond angles			
O(31)–Co(1)–O(71)	78.36(9)	O(31)–Co(2)–O(40)	87.95(10)
O(31)–Co(1)–O(80)	162.39(9)	O(31)–Co(2)–O(71)	78.51(9)
O(31)–Co(1)–N(1)	91.67(10)	O(31)–Co(2)–N(2)	166.60(10)
O(31)–Co(1)–N(11)	104.09(10)	O(31)–Co(2)–N(51)	111.20(10)
O(31)–Co(1)–N(21)	95.79(10)	O(31)–Co(2)–N(61)	94.33(11)
O(71)–Co(1)–O(80)	87.49(9)	O(40)–Co(2)–O(71)	162.87(8)
O(71)–Co(1)–N(1)	165.03(10)	O(40)–Co(2)–N(2)	102.82(10)
O(71)–Co(1)–N(11)	92.80(10)	O(40)–Co(2)–N(51)	82.10(10)
O(71)–Co(1)–N(21)	113.50(9)	O(40)–Co(2)–N(61)	86.69(11)
O(80)–Co(1)–N(1)	104.13(11)	O(71)–Co(2)–N(2)	92.18(9)
O(80)–Co(1)–N(11)	86.86(11)	O(71)–Co(2)–N(51)	92.96(10)
O(80)–Co(1)–N(21)	80.17(11)	O(71)–Co(2)–N(61)	104.60(10)
N(1)–Co(1)–N(11)	78.68(11)	N(2)–Co(2)–N(51)	78.59(11)
N(1)–Co(1)–N(21)	78.30(10)	N(2)–Co(2)–N(61)	78.57(11)
N(11)–Co(1)–N(21)	149.86(11)	N(51)–Co(2)–N(61)	151.57(11)

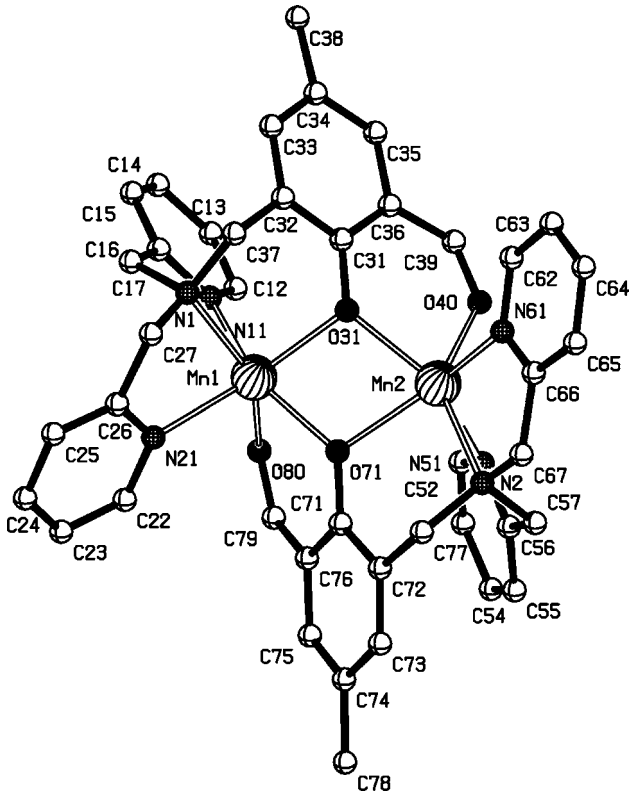

Fig. 2. Platon [17] projection of the complex cation $[Mn_2(py2ald)_2]^{2+}$. Hydrogen atoms are omitted for clarity.

are located on twofold axes. Additionally 0.7 molecule of non-coordinated methanol is present per formula unit.

3.2.2. $[Co_2(py2ald)_2](BF_4)_2 \cdot CH_3OH$ (2)

Pink hexagonal crystals of the complex were obtained by slow diethyl ether diffusion into a methanol solution of the ligand and cobalt(II) tetrafluoroborate. As the complex unit was found to be isomorphous to its perchlorate analogue, its projection is not depicted. Selected bond lengths and bond angles of compound **2** are presented in Table 2.

3.2.3. $[Mn_2(py2ald)_2](BF_4)_2 \cdot C_4H_{10}O$ (3)

Bright-yellow rod-shaped crystals of the complex were obtained by slow diffusion of diethyl ether into a methanol solution of the ligand and manganese(II) perchlorate. The Platon [17] projection of the complex is shown in Fig. 2. The selected bond lengths and angles are presented in Table 3. The complex crystallizes in the space group $P\bar{1}$ (no. 2). The unit cell includes one doubly charged complex cation, two perchlorate anions and one disordered molecule of diethyl ether. As in the case of the cobalt(II) complexes, two manganese ions are bridged by two oxygen atoms of deprotonated cresolate moieties, with a Mn1 $\cdots$ Mn2 separation of 3.4013(10) Å. Each manganese(II) ion is further coordinated by two nitrogen donor atoms of two pyridine rings, the nitrogen atom of the tertiary amino group and the oxygen atom of the aldehyde group, resulting in an extremely distorted octahedron surrounding for both metal ions. All Mn–N and Mn–O distances are in a normal range for octahedral high-spin ($S = 5/2$) manganese(II) complexes [19]. In contrast to both cobalt complexes, non-coordinated counter ions do not exhibit any disorder.

Table 3
Selected bond lengths and bond angles for $[Mn_2(py2ald)_2](ClO_4)_2C_4H_{10}O$

Bond lengths (Å)			
Mn(1)–N(11)	2.227(3)	Mn(2)–N(51)	2.214(3)
Mn(1)–N(21)	2.262(3)	Mn(2)–N(61)	2.201(3)
Mn(1)–N(1)	2.330(3)	Mn(2)–N(2)	2.374(3)
Mn(1)–O(31)	2.169(2)	Mn(2)–O(31)	2.121(2)
Mn(1)–O(71)	2.112(2)	Mn(2)–O(71)	2.194(2)
Mn(1)–O(80)	2.231(2)	Mn(2)–O(40)	2.220(3)
Bond angles			
O(31)–Mn(1)–O(71)	73.50(9)	O(31)–Mn(2)–O(40)	80.18(9)
O(31)–Mn(1)–O(80)	121.77(10)	O(31)–Mn(2)–O(71)	72.82(9)
O(31)–Mn(1)–N(1)	82.96(10)	O(31)–Mn(2)–N(2)	138.56(10)
O(31)–Mn(1)–N(11)	95.70(10)	O(31)–Mn(2)–N(51)	132.57(10)
O(31)–Mn(1)–N(21)	142.89(10)	O(31)–Mn(2)–N(61)	98.95(10)
O(71)–Mn(1)–O(80)	80.21(9)	O(40)–Mn(2)–O(71)	129.86(9)
O(71)–Mn(1)–N(1)	128.93(10)	O(40)–Mn(2)–N(2)	139.74(10)
O(71)–Mn(1)–N(11)	149.93(11)	O(40)–Mn(2)–N(51)	82.39(10)
O(71)–Mn(1)–N(21)	99.95(10)	O(40)–Mn(2)–N(61)	91.11(10)
O(80)–Mn(1)–N(1)	148.40(10)	O(71)–Mn(2)–N(2)	82.32(9)
O(80)–Mn(1)–N(11)	82.27(10)	O(71)–Mn(2)–N(51)	85.84(10)
O(80)–Mn(1)–N(21)	91.79(10)	O(71)–Mn(2)–N(61)	133.75(10)
N(1)–Mn(1)–N(11)	75.40(11)	N(2)–Mn(2)–N(51)	76.04(11)
N(1)–Mn(1)–N(21)	73.08(11)	N(2)–Mn(2)–N(61)	74.93(11)
N(11)–Mn(1)–N(21)	104.86(11)	N(51)–Mn(2)–N(61)	125.22(11)

3.3. Physical characterization

3.3.1. Mass, IR and UV–Vis spectroscopy

Electrospray mass-spectra (ESI-MS) of both cobalt(II) complexes recorded in a methanol solution reveal one major peak at m/z 405, corresponding to $[Co(py2ald)]^+$. The experimentally observed isotopic pattern is in agreement with the theoretically calculated one for $C_{21}H_{20}CoN_3O_2$. Similarly, in the ESI-MS spectrum of $[Mn_2(py2ald)_2](ClO_4)_2$ recorded in a methanol solution, a m/z 401 peak, corresponding to $[Mn(py2ad)]^+$, can be found. IR spectra of all compounds show the expected bands corresponding to the ligand and the counter ions. In particular, in all cases an intensive band at approximately 1640 cm^{-1} indicates the presence of an aldehyde group coordinated to the metal ion [20].

In the diffusion reflectance spectra of the powdered solids, for both cobalt complexes two major peaks are clearly visible. One of them, at approximately 420 nm, is a LMCT transition between the bridging phenoxo group and the metal ions and is typical for dinuclear complexes with the phenol-based deprotonated ligands [9]. The second peak, located at 1051 nm for the perchlorate complex and 1042 nm for the tetrafluoroborate complex corresponds to the $^4T_{2g} \leftarrow {}^4T_{1g}(F)$ d–d transition. In addition, in the spectra of both complexes another peak is observed at approximately 520 nm, as a shoulder of the LMCT transition band, which corresponds to the $^4T_{1g}(P) \leftarrow {}^4T_{1g}(F)$ transition. The latter two bands are typical for d–d transitions in octahedrally surrounded Co(II) ions [21]. The positions of the bands are not significantly changing if the spectra are recorded in methanol, suggesting the absence of any significant modifications in the metal coordination sphere in solution. The diffuse reflectance spectrum of $[Mn_2(py2ald)_2](ClO_4)_2$ is characterized by only one rather broad peak at 377 nm. It appears that the d–d transition band in octahedrally surrounded Mn(II) is hidden by the LMCT band from bridging phenoxo groups to the metal ions, which is usually observed around 400 nm [21]. As in the case of both cobalt complexes, no significant changes were observed when the electronic spectrum was recorded in methanol.

3.4. Magnetic susceptibility

Magnetic susceptibility measurements have been performed on crystals of **1** ($m = 16.99$ mg) and **2** ($m = 46.28$ mg) at 0.1 Tesla in the temperature range of 5–300 K. The plot of the χ^{-1} and χT versus the temperature (with χ being the magnetization per cobalt(II) ion) is shown in Fig. 3. Because the magnetic behavior of the two compounds is almost identical, only the susceptibility curve of the complex **1** is given.

At 300 K, the $\chi_1 T = 2.59$ cm^3 K mol^{-1}, which is close to the expected value for a single, uncoupled cobalt(II) ion. The value of $\chi_1 T$ decreases upon cooling, going to zero at very low temperatures. The same behavior is observed for **2**, with a value for $\chi_1 T = 2.58$ cm^3 K mol^{-1} at 300 K.

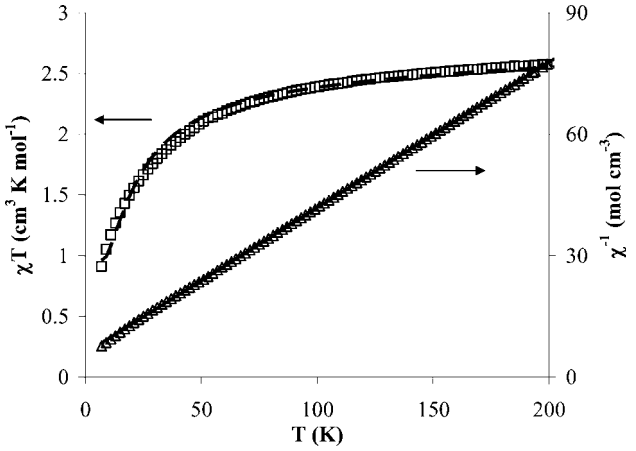

Fig. 3. χT vs. T (△) and χ^{-1} vs. T curves (□) of **1**. The solid line represents the linear fitting according to the Curie–Weiss law, the dashed line represent the calculated lines for the parameters $g_1 = 2.31$, $-J_1 = 3.56$ cm^{-1} and $\theta_1 = 3.0$ K, with $R_1 < 7.9 \times 10^{-4}$.

Fitting the linear part of the χ^{-1} versus T curve (between 50 and 300 K) results in Curie constants $C_1 = 2.63$ cm^3 K mol^{-1} and $C_2 = 2.78$ cm^3 K mol^{-1} and Curie–Weiss temperatures of $\theta_1 = -18.7$ K with $R_1 < 4.5 \times 10^{-6}$ and $\theta_2 = -16.5$ K with $R_2 < 8.7 \times 10^{-7}$. [1] The Curie constants correspond to g values of 2.36 for compound **1** and 2.43 for compound **2**.

The susceptibilities of **1** and **2** have been simulated over the entire temperature range using a modified Van Vleck equation [22,23] for a pair of coupled $S = 3/2$ spins (see Fig. 4), where $x = \exp(-J/kT)$ and N, k, β and $N\alpha$ have their normal values [24]

$$\chi = \frac{Ng^2\beta^2}{k(T-\theta)} \times \frac{14 + 5x^6 + x^{10}}{7 + 5x^6 + 3x^{10} + x^{12}} + N\alpha. \quad (1)$$

The observed and calculated susceptibilities are in agreement over the entire temperature range, applying the constants $g_1 = 2.31$, $-J_1 = 3.56$ cm^{-1} and $\theta_1 = 3.0$ K, with $R_1 < 7.9 \times 10^{-4}$, for the complex **1,** and the constants $g_2 = 2.32$, $-J_2 = 3.30$ cm^{-1} and $\theta_2 = 4.2$ K, with $R_2 < 2.6 \times 10^{-4}$ for the complex **2**.

The magnetic susceptibility of crystals of **3** (13.18 mg) has been measured between 5 and 250 K, with an external field of 0.1 Tesla. The plot of the χ^{-1} and χT versus the temperature (with χ being the magnetization per manganese(II) ion) is shown in Fig. 4. Also in this compound a decrease in magnetic susceptibility is observed with decreasing temperatures, from a value of

[1] All reliability factors for determination of the Curie–Weiss behavior have been calculated according to $R = 1/n\sum_n(\chi^{-1}_{calc} - \chi^{-1}_{obs})^2/(\chi^{-1}_{obs})^2$ and for the simulations to $R = 1/n\sum_n(\chi T_{calc} - \chi T_{obs})^2/(\chi T_{obs})^2$.

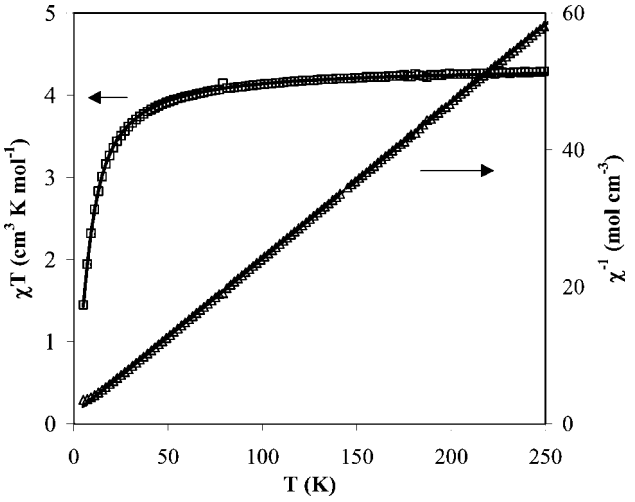

Fig. 4. χT vs. T (△) and χ^{-1} vs. T curves (□) of **3**. The solid line represents the linear fitting according the Curie–Weiss law, the dashed line represent the calculated lines for the parameters $g_3 = 1.99$, $J_3 = 0.57$ cm^{-1}, $N\alpha = 0$ and $R = 1.3 \times 10^{-5}$.

$\chi T = 4.29$ cm^3 K mol^{-1} at 250 K, to 1.4 cm^3 K mol^{-1} at 5 K. Curie–Weiss behavior above 30 K results in a Curie constant $C_3 = 4.38$ cm^3 K mol^{-1}, which corresponds to a g value of $g_3 = 2.00$.

The magnetic susceptibility fit for the dinuclear manganese(II) system based on the isotropic Heisenberg model $H = 2J\boldsymbol{S}1 \cdot \boldsymbol{S}2$ ($S1 = S2 = 5/2$) is expressed by Eq. (2) [25], where $x = \exp(-J/kT)$, and the other symbols have their usual meanings [24]. The cryomagnetic properties of **3** are simulated well by Eq. (2), using the magnetic parameters $g_3 = 1.99$, $J_3 = 0.57$ cm^{-1} and $N\alpha = 0$. The reliability factor $R = 1.3 \times 10^{-5}$

$$\chi = \frac{Ng^2\beta^2}{kT} \times \frac{x^{28} + 5x^{24} + 14x^{18} + 30x^{10} + 55}{x^{30} + 3x^{28} + 5x^{24} + 7x^{18} + 9x^{10} + 11} + N\alpha. \quad (2)$$

Acknowledgements

Support from the NRSC Catalysis (a Research School Combination of HRSMC and NIOK) is kindly acknowledged. Travel and exchange of information and students between Leiden University and Westfälische Wilhelms-Universität Münster through a NWO and DFG grant in the framework of the Joint Graduierten Kolleg is thankfully acknowledged. Also support and sponsorship concerted by COST Action D21/003/2001 is kindly acknowledged. This work was supported in part (M.L., A.L.S.) by The Netherlands Foundation for Chemical Sciences (CW) with financial aid from the Netherlands Organization for Scientific Research (NWO).

References

[1] R. Robson, Inorg. Nucl. Chem. Lett. 6 (1970) 125.
[2] D.E. Fenton, Inorg. Chem. Commun. 5 (2002) 537.
[3] K.D. Karlin, J.C. Hayes, Y. Gultneh, R.W. Cruse, J.W. McKown, J.P. Hutchinson, J. Zubieta, J. Am. Chem. Soc. 106 (1984) 2121.
[4] E. Lambert, B. Chabut, S. Chardon-Noblat, A. Deronzier, G. Chottard, A. Bousseksou, J.-P. Tuchagues, J. Laugier, M. Bardet, J.-M. Latour, J. Am. Chem. Soc. 119 (1997) 9424.
[5] N.N. Murthy, M. Mahroof-Tahir, K.D. Karlin, Inorg. Chem. 40 (2001) 628.
[6] F. Meyer, P. Rutsch, Chem. Commun. (1998) 1037.
[7] M. Suzuki, H. Kanatomi, I. Murase, Chem. Lett. (1981) 1745.
[8] P. Gamez, J. von Harras, O. Roubeau, W.L. Driessen, J. Reedijk, Inorg. Chim. Acta 324 (2001) 27.
[9] S. Torelli, C. Belle, I. Gautier-Luneau, J.L. Pierre, E. Saint-Aman, J.M. Latour, L. Le Pape, D. Luneau, Inorg. Chem. 39 (2000) 3526.
[10] T. Klabunde, C. Eicken, J.C. Sacchettini, B. Krebs, Nat. Struct. Biol. 5 (December) (1998) 1084.
[11] E.I. Solomon, U.M. Sundaram, T.E. Machonkin, Chem. Rev. 96 (1996) 2563.
[12] I.A. Koval, D. Pursche, A.F. Stassen, P. Gamez, J. Reedijk, B. Krebs, Eur. J. Inorg. Chem. 9 (2003) 1669.
[13] I.M. Kolthoff, P.J. Elving, in: Treatise on Analytical Chemistry, vol. 4, Interscience Encyclopedia, Inc, New York, 1963.
[14] P.T. Beurskens, G. Admiraal, G. Beurskens, W.P. Bosman, S. Garcia-Granda, R.O. Gould, J.M.M. Smits, C. Smykalla, The DIRDIF97 Program System, Technical Report of the Crystallography Laboratory, University of Nijmegen, The Netherlands, 1997.
[15] G.M. Sheldrick, SHELXS 97, Program for Crystal Structure Refinement, University of Göttingen, Germany, 1997.
[16] H.D. Flack, Acta Crystallogr. A 39 (1983) 876.
[17] A.L. Spek, J. Appl. Crystallogr. 36 (2003) 7.
[18] H. Adams, D.E. Fenton, S.R. Haque, S.L. Health, M. Ohba, H. Okawa, S.E. Spey, J. Chem. Soc., Dalton Trans. (2000) 1849.
[19] G. Wilkinson (Ed.), Comprehensive Coordination Chemistry, vol. 5, Pergamon Press, Toronto, 1987.
[20] K. Nakamoto, Infrared and Raman Spectra of Inorganic and Coordination Compounds, Wiley, New York, 1986.
[21] A.B.P. Lever, in: Inorganic Electronic Spectroscopy, vol. 33, Elsevier, Amsterdam, 1984.
[22] S. Emori, H. Nakashima, W. Mori, Bull. Chem. Soc. Jpn. 73 (2000) 81.
[23] A. Earnshow, Introduction to Magnetochemistry, Academic Press, London, 1968.
[24] O. Kahn, Molecular Magnetism, Wiley-VCH, New York, 1993.
[25] H. Sakiyama, A. Sugawara, M. Sakamoto, K. Unoura, K. Inoue, M. Yamasaki, Inorg. Chim. Acta 310 (2000) 163.